ISSN 1063-7710, Acoustical Physics, 2014, Vol. 60, No. 1, pp. 110–114. © Pleiades Publishing, Ltd., 2014.

ACOUSTIC SIGNAL PROCESSING AND COMPUTER SIMULATION

Multi-Splitting of Lamb Waves Band Gap in One-Dimensional Quasi-Periodic Plates of Cantor Series[1]

Hong-Xing Ding[a, b], Li-Li Dai[b], Zhong-Hua Shen[a], Lin Yuan[a], and Xiao-Wu Ni[a]

[a] *School of Science, Nanjing University of Science and Technology, Lianyungang, 222006 China*

[b] *Department of Physics, Lianyungang Teachers College, Lianyungang, 222006 China*

e-mail: shenzh@mail.njust.edu.cn, dinghxing@126.com

Received May 14, 2013

Abstract—We study numerically the propagation of Lamb waves in one-dimensional (1D) quasi-periodic composite thin plates consisting of a row of air holes embedded in the matrix material silicon according to a Cantor sequence; the surfaces of the plate are parallel to the axis of quasi-periodicity. The phenomenon of multi-splitting in the band gap structures is demonstrated. A semi-quantitative explanation is proposed in which the inherent cavity-like structure is proven to play the essential role in the phenomenon of multi-splitting, which gives a reliable way to predict where and how the band gap is splitting in the quasi-periodic systems. Possible applications are discussed.

Keywords: Lamb waves, phononic crystals, band gap splitting

DOI: 10.1134/S1063771014010059

1. INTRODUCTION

Over the past decade, propagation of Lamb waves in phononic crystal (PC) plates has received much attention because of their renewed physical, chemical and biological applications [1–12]. Since the elastic wave energy is absolutely confined between the two stress-free boundaries [1], Lamb waves can support long distance propagation which makes it more interesting than that of bulk and surface acoustic wave. By the results of experimental measurement of the Lamb waves' amplitude at the fundamental frequency, the spatial distributions of the quadratic and cubic nonlinear acoustic parameters can be calculated [2]. Moreover, Lamb waves device is easier to scale down in size, therefore the related researches have proved the existence of large complete band gaps at high frequencies in the PC membranes, which may open up another dimension in design and implementation of acoustic devices for wireless and sensing applications [3, 4].

The study of Lamb wave propagation in composite plates starts from the periodical structures for which one of most noted characteristics should be the band gap structures. The theoretical work begins by Chen et al., who have employed a rigorous theory of elastic wave to demonstrate the existence of band gaps for lower-order Lamb waves modes in 1D periodical PC plate [5]. Gao et al. have studied the substrate effect on the band gap structures of lower-order Lamb waves and shown that a new band gap is formed in lower frequency range due to inter-mode coupling and repelling [6]. Zhang et al. have demonstrated the existence of Lamb waves band gaps in the PCs manufactured by patterning periodical air-filled holes in thin plates through laser ultrasonic measurements [7]. Besides the studies of Bragg-scattering-based PC plates mentioned above, band gaps and waveguide of Lamb waves in the locally resonant PC plates were also investigated both numerically and experimentally for its potential applications in low-frequency range [8–12]. Recently, Lamb waves propagation in quasi-periodic composite plates has received more attention in the community of PC researchers. Gao et al. [13] have discovered the phenomena of single splitting of the band gap structures in 1D two-component Fibonacci quasi-periodic composite plates and then Chen et al. studied the splitting in the three-component case [14]. Chen et al. have pointed out that the Lamb waves band-gap in 1D PCs can be substantially enlarged by using the combination of periodic and Fibonacci quasi-periodic composite thin plates [15].

In our work, the Cantor series configuration is investigated as an interesting example, which has been extensively studied in other wave systems [16–19]. Additionally, in condense physics, the wave spectra of Cantor series system shows an interesting characteristic of self-similarity, which has recently been demonstrated in the kinetic and stochastic counterpart of thetriadic Cantor set [20]. We have numerically studied the Lamb wave propagating in 1D quasi-periodic plates of Cantor series and observed the phenomena of

[1] The article is published in the original.

multi-splitting in the band gap structures. A semi-quantitative explanation is given, in which the inherent cavity-like structure is demonstrated to play the essential role in the band gap multi-splitting and self-similarity. It should be mentioned that the theoretical explanation also holds for other kind of quasi-periodic systems, which gives a reliable way to predict where and how the band gap is splitting, and is very significant in the application of nondestructive diagnosis and integrated Lamb wave devices, such as multi-channel filters.

2. THE THEORETICAL MODEL

As shown by Fig. 1, the composite thin PC plate consists of a row of air holes of radius r embedded quasi-periodically in the matrix material silicon, the surfaces of the plate being parallel to the axis of quasi-periodicity. The thickness of the plate is L and the width of the component A (with air hole) and component B are d_A and d_B, respectively. Where the sequence order of A and B is arranged in the Cantor series. One can obtain the quasi-periodic system of the Cantor series according to the production rule $S_n = S_{n-1}B_nS_{n-1}$ for $n \geq 1$ with $S_0 = A$ and $S_1 = ABA$. Here, the generation number $n = 3$ (layer number: $N = 27$); A and B are identical in structural dimensions, *viz.* $d_A = d_B$ (lattice spacing; $D = d_A + d_B$). The Lamb waves propagate along the x direction and the perfectly matching layer (PML) is coated on both ends of the plate. Since a two-dimensional problem is considered in this paper, all field components are y-independent.

To demonstrate the multi-splitting in band gap structures of Cantor series comparing to that of periodic systems, we calculate transmitted power spectra (TPS) by using finite element method (FEM) [21–23]. In the numerical simulations, the Lamb waves are supposed to be excited by a periodic laser pulse which is perpendicular to the surface of the plate, and the exciting position is close to the corrugated region. The elastic constants of silicon (crystalline orientation index: <100>) are $C^{11} = 1.66 \times 10^{11}$, $C^{12} = 6.39 \times 10^{10}$, $C^{44} = 7.96 \times 10^{10}$ (in units of N/m^2), mass density $\rho = 2.331 \times 10^3$ kg/m^3; the elastic constants of air are $C^{11} = 1 \times 10^6$, $C^{12} = 0$, $C^{44} = 1 \times 10^6$ (in units of N/m^2), mass density $\rho = 1 \times 10^{-4}$ kg/m^3. The plate thickness $L = 0.5$ mm, the radius of air holes $r = 0.2$ mm and the width of unit A (or B) is d_A (or d_B) $= 0.5$ mm. The excited Lamb waves are supposed to be totally absorbed by the PMLs coated on both plate ends.

3. NUMERICAL RESULTS AND DISCUSSIONS

Figure 2 gives TPS for the periodic and quasi-periodic plates with $L/D = 0.5$. For the periodic system, there exists only one band gap from frequency of 1814 up to 3800 kHz. However, for the quasi-periodic system, multi-splitting is seen in this band gap, and a new one appears in contiguous lower-frequency range about of 1520 to 1810 kHz. One can observe that nine splitting peaks occur in the band gap structure and the splitting peaks are marked by A, B, C, D, E, F, G, H and I [A (1927850 Hz), B (24443878 Hz), C (2485350 Hz), D (2493700 Hz), E (2548450 Hz), F (2731750 Hz), G (2978300 Hz), H (3267753 Hz), I (3510450 Hz)], respectively. The calculation step of B and H is 0.1 Hz and the others are 50 Hz.

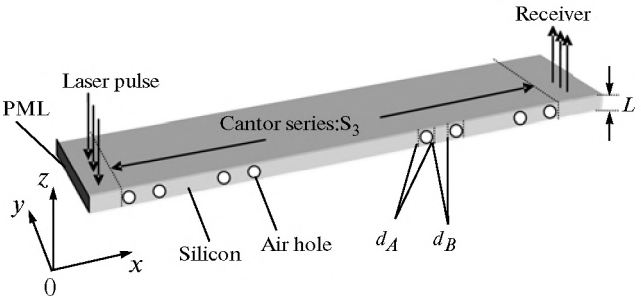

Fig. 1. The schematic diagram of 1D Cantor quasi-periodic PC plates. Perfectly matching layer (PML) is coated on both ends of the plate.

In order to study the nature of the band gap splitting phenomenon, we further calculate the displacement fields of the PC plate under the corresponding exciting frequencies as shown in Figs. 3a–3i. The results demonstrate that the splitting peaks are caused by the cavities inherent in Cantor series system, and the cavity-like structures can be classified into two categories, *viz.* *ABA*[3*B*]*ABA* and *ABA*[9*B*]*ABA*. Therefore, when a specific Lamb wave mode is captured by the cavity, the wave energy is accumulated rapidly due to the resonating effect which finally leads to the penetration through scatters barrier, *viz.* *ABAB*..., for the selected mode. And the physical instinct of band gap splitting is that the working frequency of the selected Lamb wave mode is coincidentally positioned in the band gap of the periodic counterpart. Here it needs to mention that when the quasi-periodic generation number n increases, the characteristic cavity-like structures would only emerge repeatedly, so the band gap splitting is supposed to be independent with the layer number N which is also demonstrated numerically by Gao et al. [13]. In the enlarged plots of deformed shape, it is interesting to find out that the two peak sets (A, B, F, G, I and C, D, E, H) in TPS have different physical origins, in which the set (A, B, F, G, I) stems from the resonating selection of lower-order anti-symmetric modes (A_0) and the set (C, D, E, H) from the resonating selection of lower-order symmetric modes (S_0). The two modes are decoupled when Lamb waves propagate in a plate with a mirror plane [16]. This property is meaningful in the applica-

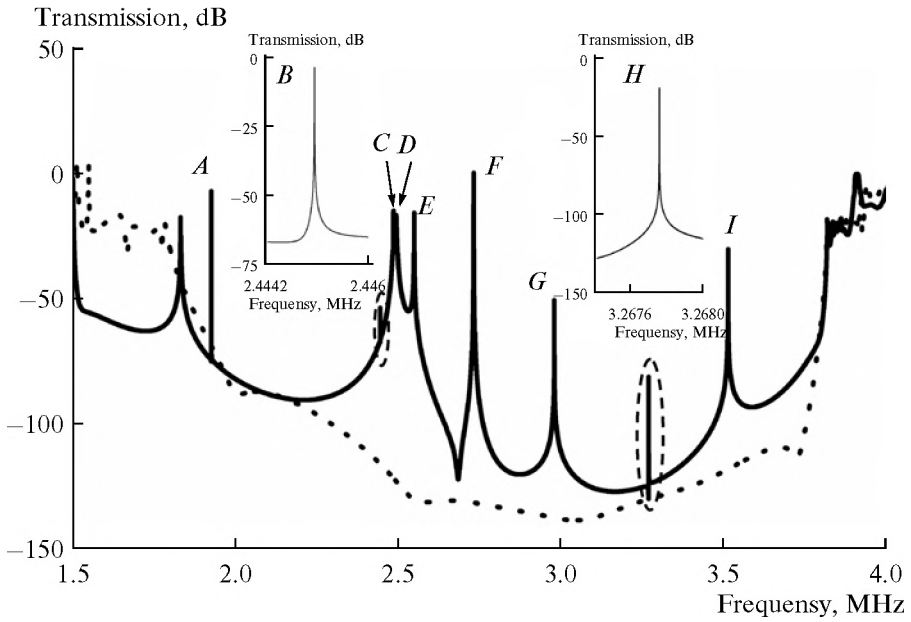

Fig. 2. TPS for the periodic plate (dotted line) and the quasi-periodic (Cantor series) plate (solid line) with the calculation step of 50 Hz. The inserted TPS is high accuracy one with the calculation step of 0.1 Hz for splitting peaks B and H indicated by the elliptic circle (dashed line).

tion of nondestructive diagnosis due to the fact that defects in the plate can easily cause mode conversion ($A_0 \rightarrow S_0$ or $S_0 \rightarrow A_0$). However, in order to give where the splitting peaks locate, one has to know not only the mode type but also the Bloch wavelength of each resonating Lamb wave mode. In Figs. 3a–3i, the ruler is marked to show Bloch wavelength of the resonating Lamb wave mode in the cavity in millimeter, the Bloch wavelength is $\lambda_a \approx 1.65$ mm for the peak A; $\lambda_b \approx 1.4$ mm for the peak B; $\lambda_{c,d,e} \approx 3$ mm for the peak C, D and E; $\lambda_f \approx 1.3$ mm for the peaks F; $\lambda_g \approx 1.23$ mm for the peaks G; $\lambda_h \approx 2.3$ mm for the peaks H; $\lambda_i \approx 1.1$ mm for the peaks I. The corresponding reduced wave number is then $\hat{k}_a \approx 0.61$ for the peak A; $\hat{k}_b \approx 0.71$ for the peak B; $\hat{k}_{c,d,e} \approx 0.33$ for the peak C, D and E; $\hat{k}_f \approx 0.77$ for the peaks F, $\hat{k}_g \approx 0.81$ for the peaks G, $\hat{k}_h \approx 0.43$ for the peaks H, $\hat{k}_i \approx 0.91$ for the peaks I, calculated by the equation $\hat{k} = kD/\pi = D/\lambda$.

The dispersion curve of a pure silicon plate (thickness: $L = 0.5$ mm) is drawn in Fig. 4, in which nine points are marked to predict the positions of splitting peaks in the frequency domain. For points A, B, F, G and I, the corresponding reduced wave number is nearby 0.61, 0.71, 0.77, 0.81 and 0.91 respectively with the mode type to be A_0. For points C, D, E and H, the reduced wave number is nearby 0.33 and 0.43 with the mode type to be S_0. From the chart, one can obtain that the predicted position of each splitting peak is around 1936 kHz for peak A; around 2462 kHz for peak B; around 2536 kHz for peaks C, D and E, around 2787 kHz for peak F; around 3008 kHz for peak G; around 3291 kHz for peak H; around 3569 kHz for peak I; which are in very good agreement with the results in TPS of Fig. 2.

4. CONCLUSION

In conclusion, we have demonstrated the phenomena of multi-splitting in the band gap structures of Cantor series systems. A semi-quantitative explanation is given, in which the inherent cavity-like structure, *viz.* *ABA*[3*B*]*ABA* and *ABA*[9*B*]*ABA*, is proven to play the essential role in the band gap multi-splitting, which gives a reliable way to predict where and how the band gap is splitting, and is very significant in the application of nondestructive diagnosis and integrated Lamb wave devices, such as multi-channel filters.

Finally, we are thankful to the Acoustical Physics for the free access retrieval system lodged in the Internet (see http://www.akzh.ru/rubrics_en.htm) [24]. One can easily find the list of adjoining papers which is too large for citing in References. For example, the last paper on Lamb waves published in Acoustical Physics is [25].

Authors would like to thank the financial support of this research from the National Science Foundation of

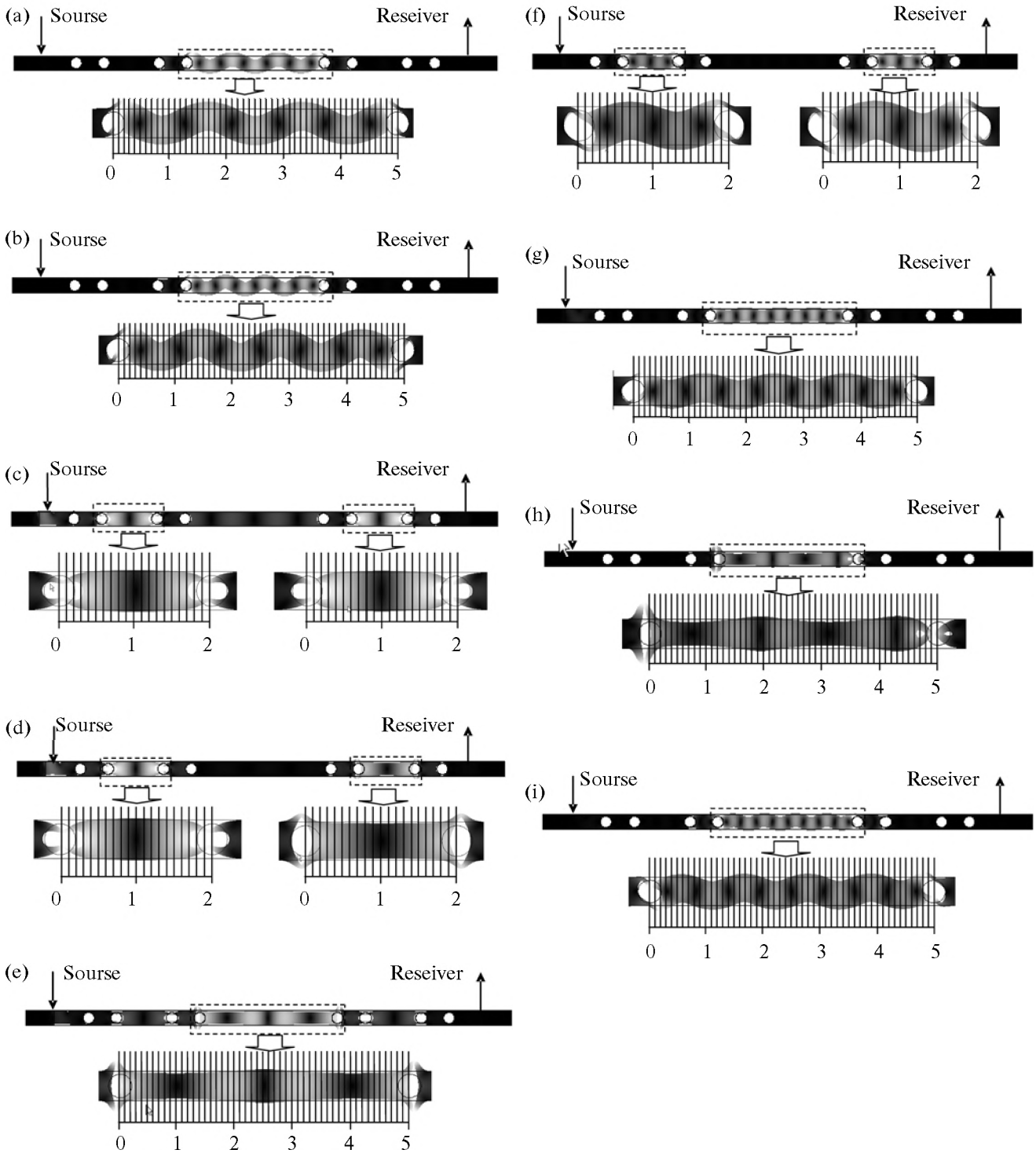

Fig. 3. The displacement fields at the frequency loads of (a) 1927850 Hz, (b) 24443878 Hz, (c) 2485350 Hz, (d) 2493700 Hz, (e) 2548450 Hz, (f) 2731750 Hz, (g) 2978300 Hz, (h) 3267753 Hz and (i) 3510450 Hz, respectively. Corresponding plot in each figure is enlarged, and the ruler is marked to show Bloch wavelength of the resonating Lamb wave mode in the cavity in millimeter.

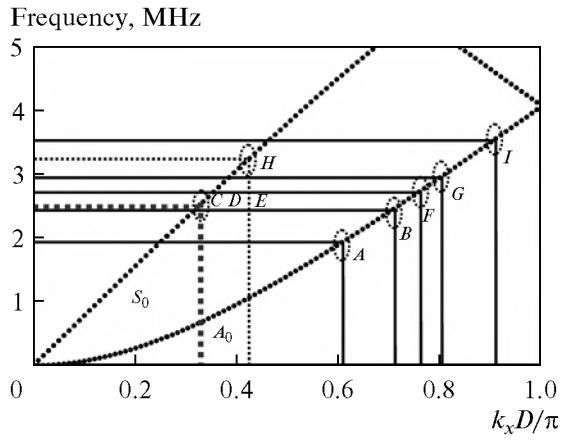

Fig. 4. The dispersion curve of a pure Silicon plate (thickness: $L = 0.5$ mm). Nine points are marked to show where the positions of splitting peaks should be in the frequency domain.

China under nos. 11274175 and 61108013, and the Jiangsu Province College Qing Lan Project.

REFERENCES

1. A. I. Korobov and M. Yu. Izosimova, Acoust. Phys. **52**, 589 (2006).
2. M. Yu. Izosimova, A. I. Korobov, and O. V. Rudenko, Acoust. Phys. **55**, 153 (2009).
3. S. Mohammadi, A. A. Eftekhar, A. Khelif, W. D. Hunt, and A. Adibi, Appl. Phys. Lett. **92**, 221905 (2008).
4. S. Mohammadi, A. A. Eftekhar, W. D. Hunt, and A. Adibia, Appl. Phys. Lett. **94**, 051906 (2009).
5. J.-J. Chen, K.-W. Zhang, J. Gao, and J.-C. Cheng, Phys. Rev. B: Condens. Matter Mater. Phys. **73**, 094307 (2006).
6. J. Gao, X.-Y. Zou, J.-C. Cheng, and B. Li, Appl. Phys. Lett. **92**, 023510 (2008).
7. X.-Y. Zhang, T. Jackson, and E. Lafond, Appl. Phys. Lett. **88**, 041911 (2006).
8. A. Khelif, P. A. Deymier, B. Djafari-Rouhani, J. O. Vasseur, and L. Dobrzynski, J. Appl. Phys. **94**, 1308 (2003).
9. J.-C. Hsu and T.-T. Wu, Appl. Phys. Lett. **90**, 201904 (2007).
10. J.-H. Sun and T.-T. Wu, Phys. Rev. B: Condens. Matter Mater. Phys. **76**, 104304 (2007).
11. T.-C. Wu, T.-T. Wu, and J.-C. Hsu, Phys. Rev. B: Condens. Matter Mater. Phys. **79**, 104306 (2009).
12. M. Oudich, Y. Li, B. M. Assouar, and Z.-L. Hou, New J. Phys. **12**, 083049 (2010).
13. J. Gao and J.-C. Cheng, Appl. Phys. Lett. **90**, 111908 (2007).
14. J.-J. Chen, B. Qin, and H. L. W. Chan, Solid State Commun. **146**, 491 (2008).
15. J.-J. Chen, Q. Wang, and X. Han, Phys. Lett. B **24**, 161 (2010).
16. N.-H. Liu, W.-G. Feng and X. Wu, J. Phys. **5**, 4623 (1993).
17. M. S. Vasconcelos and E. L. Albuquerque, Physica B: Condensed Matter **222**, 113 (1996).
18. D. L. Jaggard and A. D. Jaggard, Optics Letters **22**, 145 (1997).
19. J. R. Mejia-Salazar, N. Porras-Montenegro, E. Reyes-Gomez, S. B. Cavalcanti and L. E. Oliveira, Europh. Lett. **95**, 24004 (2011).
20. M. K. Hassan, M. Z. Hassan, N. I. Pavel, arXiv.org, cond-mat, arXiv: 0907, 4837 (2009).
21. X.-F. Zhu, T. Xu, S. C. Liu, and J.-C. Cheng, J. Appl. Phys. **106**, 104901 (2009).
22. X.-F. Zhu, X.-Y. Zou, B. Liang, and J.-C. Cheng, J. Appl. Phys. **108**, 124909 (2010).
23. H.-X. Ding, Z.-H. Shen, J. Jia, and X.-W. Ni, Acoust. Phys. **57**, 866 (2011).
24. V. G. Shamaev, A. B. Gorshkov, and A. V. Zharov, Akust. Zh. **59**, 283 (2013).
25. A. D. Lapin, Acoust. Phys. **59**, 267 (2013).